24th INTERNATIONAL CONGRESS ON SOUND AND VIBRATION
23–27 July 2017, London

# RESEARCH ON DYNAMIC MODELING AND VIBRATION CHARACTERISTICS OF RIGID-FLEXIBLE COUPLING ROTATING BLADE

Yaliu Yang and Guangcai Han

*Harbin Engineering University, College of Aerospace Engineering and Civil Engineering, Harbin, HeiLongJiang, China.*
*email: yangyaliu@outlook.com*

Noise of propeller is induced by the vibration of blade. Dynamic analysis of the rotating blade is very important to predict its vibration characteristics. Based on the Hamilton's principle, dynamic equations of a rotating blade were established and discretized by finite element method. Meanwhile, on the condition of blade bending deformation, the potential energy of axial shortening caused by gravity and centrifugal force was calculated in the equations. Moreover, numerical simulation of the equations was achieved by using MATLAB with the method of Newmark integration. On these bases, this paper studied the blade vibration characteristics on different length and rotational speed, investigated the effects of variable and pre-twist variable cross-section on blade vibration characteristics. The results showed that with the increase of blade rotation speed and the length of blade, the displacement and velocity response of blade tip was increased, the bending degree of vibration curve became greater. In addition, considering the blade weight and pre-twisted angle, the displacement and velocity response of blade tip were smaller, same result was obtained by the bending degree of vibration curve. Furthermore, the effects on the displacement and velocity response of blade tip along with the first-order and second-order vibration mode were investigated in detail，which were caused by the change of blade weight as well as the diameter of rigid disk. Rigid-flexible coupling dynamic models and equations were given in this paper in consideration of the rotating blade weight. Furthermore, the vibration characteristics of propeller blade were studied. Equations and simulation results derived in this paper have a theoretical significance and engineering value.

Keywords: pre-twisted rotating blade, rigid-flexible coupled, dynamics simulation, blade vibration

## 1. Introduction

The vibration characteristics analysis of rotating cantilever beam is very important in mechanical engineering, most engineering examples can be idealized as rotating cantilever beam. In order to make the design of the rotating blade structure more reasonable, the vibration characteristics of the blade need to be more scientific and more accurately calculated. Compared to the non-rotating structure, the vibration characteristics of the rotating structure change is very obvious, because of this, the dynamic characteristics of rotating blades has been studied extensively.

The study of natural frequencies of rotating beams originates from Southwell [1] and Gough. Based on the Rayleigh energy theorem, they propose a simple equation, the famous Southwell equation[2], which is still widely used by many engineers at now. Later, Ansari [3] studied the nonlinear dynamics of a non-uniform asymmetric section rotating blade with a pre-torsion angle mounted on a rotating disk. Although considering the nonlinear factor issue from Coriolis force, which caused by rotation of the blade, the axial deformation of the blade was ignored. With the development of com-

puter and digital methods, Yokoyamals [4] studied the free vibration of rotating Timoshenko beam based on Hamilton principle, he used the finite element method to discretize the research object and studied the effects of the pre-twist angle, the shearing deformation and the moment of inertia on the vibration behaviour of the blades. Meanwhile, the British scholar J. R. Banerjee [5] studied the vibration characteristics of the variable cross-section rotating beam. Furthermore, by using the finite element method, Jianjun Wang analysed the dynamic characteristics of a typical rotating blade, including the frequency of the steering, vibration mode conversion and other issues.

In this paper, based on the second Lagrange equations, finite element method was adopted to establish rigid-flexible coupling discrete dynamic equations of a rotating blade. The effects of physical factors such as blade rotational speed on the dynamic behaviour of the rotating blades were investigated. The dynamic properties of the rotating blades with equal cross-section and variable cross-section were analysed and compared. The formulas and numerical simulation results are of theoretical and engineering value. The computer simulation results have a certain theoretical significance and some applied value in engineering.

## 2. Kinetic equations

Three coordinate systems were given in Fig.1.The inertial reference system $oXYZ$ .The moving coordinate system $ox_1y_1z_1$ was fixed on the disc and rotated at angular velocity $\dot{\varphi}$. The moving coordinate system $oxyz$ was fixed on the blade. The center of the disc is denoted as $o$. The blade was divided into n units, the i-th unit of the node number was $i$ and $i+1$, the location of the i-th unit in $ox_1y_1z_1$ was represented by $L_i$.

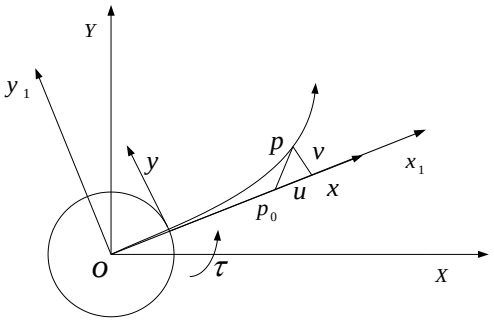


Figure 1: Disc – blade mechanical model displacement field

According to the theory of Euler-bernoulli beam, the kinetic energy of the blade element was calculated as follows:

Assuming the point on the neutral axis of the n-th element blade before deformation was $p_0$, after the deformation point with $p$ .Then the position vector could be expressed as[6]

$$R_p = \left[A(\varphi)\right] r_p \tag{1}$$

$$r_p = \begin{bmatrix} L_i + x \\ v(x,t) \end{bmatrix} \tag{2}$$

$$Li = (i-1)\frac{L}{n} \tag{3}$$

$$\left[A(\varphi)\right] = \begin{bmatrix} \cos\varphi & -\sin\varphi \\ \sin\varphi & \cos\varphi \end{bmatrix} \tag{4}$$

According to above equations, we could get

$$\dot{R}_p = \left[A(\varphi)\right]\dot{r}_p + \dot{\varphi}\left[A_\varphi(\varphi)\right] r_p \tag{5}$$

In the inertial system， we could get

$$\dot{R}_p = \begin{bmatrix} -\alpha \sin\varphi - \beta \cos\varphi \\ \alpha \cos\varphi - \beta \sin\varphi \end{bmatrix} \tag{6}$$

$$\alpha = \dot{v} + \dot{\varphi}(L_i + x) \tag{7}$$

$$\beta = \dot{\varphi} v \tag{8}$$

Assuming the per unit quality of the blade length as $\rho$ ,the i-th unit kinetic energy of the blade could be written as

$$T_i = \frac{1}{2}\int_0^l \rho \dot{R}_p^T \dot{R}_p dx = \frac{1}{2}\int_0^l \rho \left[ \dot{v}^2 + 2\dot{\varphi}(L_i + x)\dot{v} + \dot{\varphi}^2 v^2 + \dot{\varphi}^2 (L_i + x)^2 \right] dx \tag{9}$$

The unit potential energy of the blade was calculated as follows

$$V_{bi} = \frac{1}{2}\int_0^l EI \left( \frac{\partial^2 v}{\partial x^2} \right)^2 dx \tag{10}$$

The axial shortening caused by the lateral bending deformation of the blade was

$$du = -\frac{1}{2}\left( \frac{\partial v}{\partial x} \right)^2 dx \tag{11}$$

The axial inertial force and weight component acting on the i-th element surface were

$$\begin{aligned} F_p &= \int_x^l \rho[-\dot{\varphi}^2 (L_i + x)]dx + \sum_{j=i+1}^{n} \rho_j l_j \left[ -(L_j + \frac{l_j}{2})\dot{\varphi}^2 \right] \\ &= -\rho\dot{\varphi}^2 \left[ L_i (l - x) + \frac{1}{2}(l^2 - x^2) \right] + \sum_{j=i+1}^{n} \rho_j l_j \left[ -(L_j + \frac{l_j}{2})\dot{\varphi}^2 \right] \end{aligned} \tag{12}$$

$$F_{mg} = \int_x^l \rho g \sin\varphi dx + \sum_{j=i+1}^{n} \rho_j l_j g \sin\varphi \tag{13}$$

The i-th unit potential energy of the blade was[7]

$$\begin{aligned} V_{ai} &= \int_0^l F_p du + \int_0^l F_{mg} du \\ &= \frac{1}{2}\int_0^l \left\{ \rho \left[ L_i \dot{\varphi}^2 (l - x) + \frac{1}{2}\dot{\varphi}^2 (l^2 - x^2) \right] \left( \frac{\partial v}{\partial x} \right)^2 \right\} dx + \frac{1}{2}\int_0^l \left\{ \sum_{j=i+1}^{n} \rho_j l_j \left[ (L_j + \frac{l_j}{2})\dot{\varphi}^2 \right] \left( \frac{\partial v}{\partial x} \right)^2 \right\} dx \\ &\quad -\frac{1}{2}\int_0^l \left\{ \rho g \sin\varphi (l - x) \left( \frac{\partial v}{\partial x} \right)^2 \right\} dx + \frac{1}{2}\int_0^l \left\{ \sum_{j=i+1}^{n} \rho_j l_j g \sin\varphi \left( \frac{\partial v}{\partial x} \right)^2 \right\} dx \end{aligned} \tag{14}$$

By using finite element method, the bladewas discretized as

$$v(x,t) = [N(x)]\{q(t)\} \tag{15}$$

$$V_{bi} = \frac{1}{2}\{q\}^T \int_0^l EI[N'']^T [N'']dx\{q\} \tag{16}$$

$$
\begin{aligned}
V_{ai} = \frac{1}{2} L_i \dot{\varphi}^2 \{q\}^T \int_0^l \rho [N']^T [N'](l-x)dx\{q\} + \frac{1}{4}\dot{\varphi}^2 \{q\}^T \int_0^l \rho [N']^T [N'](l^2 - x^2)dx\{q\} \\
+ \frac{1}{2}\sum_{j=i+1}^{n} l_j (L_j + \frac{l_j}{2})\dot{\varphi}^2 \{q\}^T \int_0^l \rho_j [N']^T [N']dx\{q\} \\
- \frac{1}{2}\{q\}^T \int_0^l \rho g \sin\varphi [N']^T [N'](l-x)dx\{q\} \\
- \frac{1}{2}\sum_{j=i+1}^{n} l_j g \sin\varphi \{q\}^T \int_0^l \rho_j [N']^T [N']dx\{q\}
\end{aligned} \tag{17}
$$

Assuming

$$
\begin{aligned}
[M] &= \int_0^l \rho [N]^T [N]dx \\
[K] &= \int_0^l EI [N'']^T [N'']dx \\
[k_{a1}] &= \int_0^l \rho [N']^T [N'](l-x)dx \\
[k_{a2}] &= \int_0^l \rho [N']^T [N'](l^2 - x^2)dx \\
[k_{a3}] &= \int_0^l \rho_j [N']^T [N']dx \\
[a] &= \int_0^l \rho [N]dx \\
[b] &= \int_0^l \rho x [N]dx
\end{aligned} \tag{18}
$$

The kinetic and potential energy of a unit can be expressed as

$$
T_i = \frac{1}{2}\rho l \dot{\varphi}^2 \left( L_i^2 + \frac{l^2}{3} + L_i l \right) + \frac{1}{2}\{\dot{q}\}^T [M]\{\dot{q}\} + \dot{\varphi}[L_i[a] + [b]]\{\dot{q}\} + \frac{1}{2}\dot{\varphi}^2 \{q\}^T [M]\{q\} \tag{19}
$$

$$
\begin{aligned}
V_i = \frac{1}{2}\{q\}^T [K]\{q\} + \frac{1}{2} L_i \dot{\varphi}^2 \{q\}^T [k_{a1}]\{q\} + \frac{1}{4}\dot{\varphi}^2 \{q\}^T [k_{a2}]\{q\} \\
+ \frac{1}{2}\sum_{j=i+1}^{n} l_j (L_j + \frac{l_j}{2})\dot{\varphi}^2 \{q\}^T [k_{a3}]\{q\} - \frac{1}{2} g \sin\varphi \{q\}^T [k_{a1}]\{q\} - \frac{1}{2}\sum_{j=i+1}^{n} l_j g \sin\varphi \{q\}^T [k_{a3}]\{q\}
\end{aligned} \tag{20}
$$

According to the Lagrange equation [8]

$$
\frac{d}{dt}\frac{\partial (T_i - V_i)}{\partial \{\dot{q}\}} - \frac{\partial L_i}{\partial \{q\}} = \{F\} \tag{21}
$$

The unit dynamic equation of blade was obtained

$$
\begin{aligned}
[M]\{\ddot{q}\} + \Bigg[ [K] + \left( L_i \dot{\varphi}^2 - g\sin\varphi \right)[k_{a1}] + \frac{1}{2}\dot{\varphi}^2 [k_{a2}] \\
+ \sum_{j=i+1}^{n} l_j \left[ \dot{\varphi}^2 (L_j + \frac{l_j}{2}) - g\sin\varphi \right][k_{a3}] - \dot{\varphi}^2 [M] \Bigg] \{q\} + \ddot{\varphi}\left[ L_i[a] + [b] \right]^T = 0
\end{aligned} \tag{22}
$$

Considering the case of variable cross-section, the moment of inertia of the section would vary with the coordinate

$$I = \frac{b_1 h_1^3}{12} - \frac{b_2 h_2^3}{12} \tag{23}$$

When the pre-twist angle was considered, the moment of inertia was formed as

$$I = I_x \cos^2\theta + I_y \sin^2\theta \tag{24}$$

## 3. Dynamic simulation

In this paper, numerical simulation was done by MATLAB, the dynamic behaviour of the rotating blades was shown and visualized.

As illustrated in Fig.2, assuming the blade length as $34\,m$, $\rho$=1760kg/m$^3$, $b_1 = 0.6m$, $h_1 = 0.19m$, $b_2 = 0.4m$, $h_2 = 0.17m$, Elastic Modulus $E$=$4\times10^{11}\,pa$, rotating speed was $61r/\min$, the diameter of the rigid disc was $1.5m$.

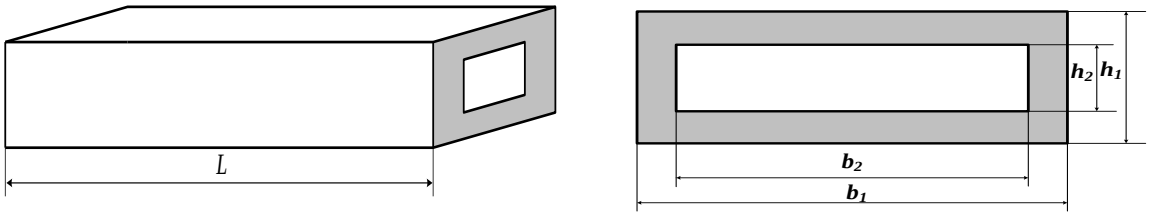


(a) Shape of the blade (b) Cross-sectional dimension

Figure 2: Dimensions of the blades

In the case of different rotating speed (blue line:$64\,r/\min$, red line:$61\,r/\min$, black line:$58\,r/\min$), we can get the following simulation results.

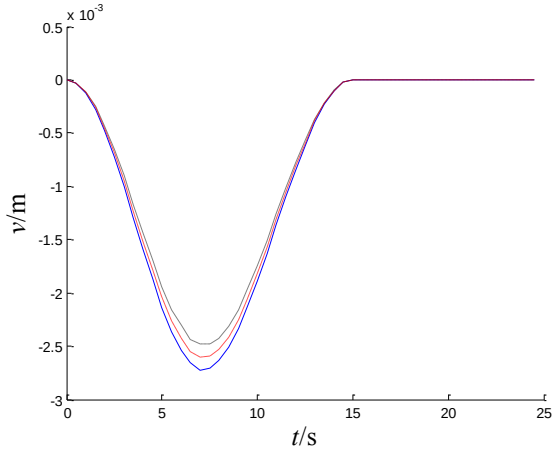


Figure 3: Displacement response of blade tip

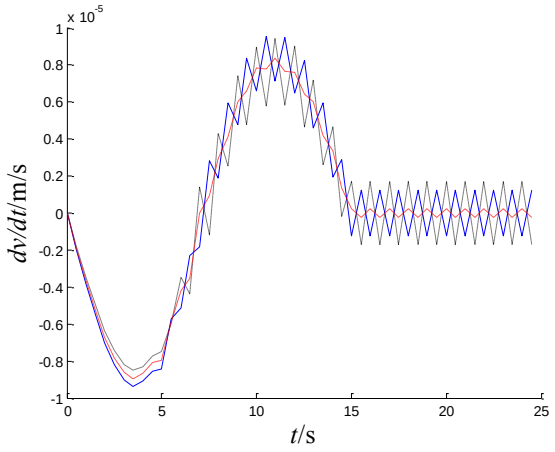


Figure 4: Speed change of blade tip

From Fig.3 , with the increase of the rotational speed, we can get that the maximum displacement of the blade tip was increased, the basic reason was that the rotation angle and rotation speed were related to the stiffness matrix of the system, and the change of the rotation speed affected the stiffness matrix of the dynamic equation. From Fig.4, we can see that the rotational speed $61\,r/\min$ was most suitable.

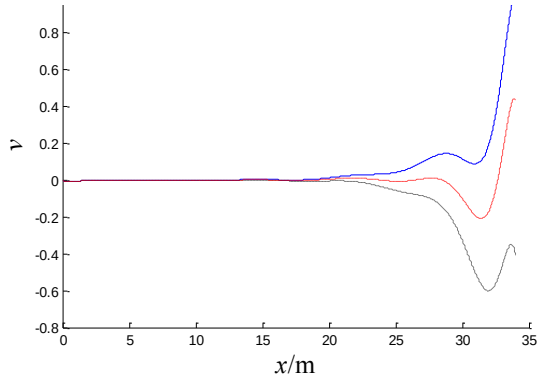


Figure 5: First modal shape chart

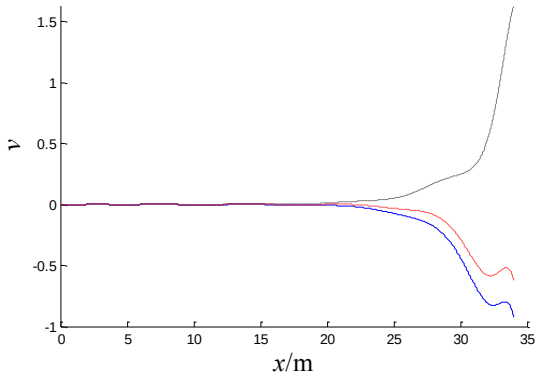


Figure 6: Two classes mode shapes chart

At the rotational speed 61 $r/\min$, the vibration curve was near the vibration axis and did not deviate very far compared to the other two conditions. This indicated that the rotating speed should not be too large nor too small, it was depending on the actual situation.

When the cross-sectional area changed, assuming the blade length as 34 $m$, $\rho$=1760kg/m$^3$, $b_{01}$=0.6$m$, $b_{02}$=0.4$m$, $b_{11}$=0.575$m$, $b_{12}$=0.375$m$, $h_1$=0.17$m$, $h_2$ = 0.15$m$, $E$=4×10$^{11}$ $pa$

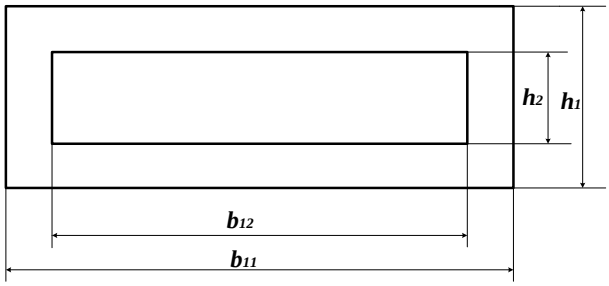


Figure 7: $B_1$-*size* of the variable cross-section blade

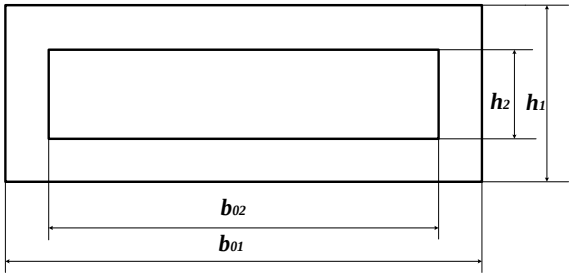


Figure 8: $B_2$-*size* of the variable cross-section blade

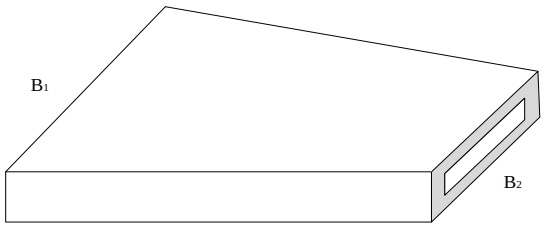


Figure 9: Shape of the variable cross-section blade

We can get the simulation result as below.( blue line: equal section blade, red line: variable cross-section blade)

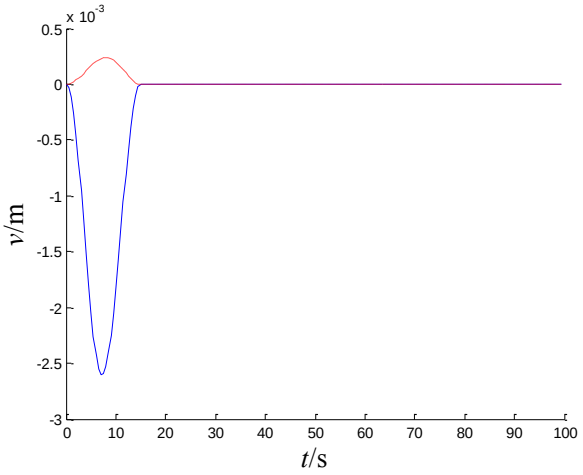


Figure 10:Displacement response of blade tip

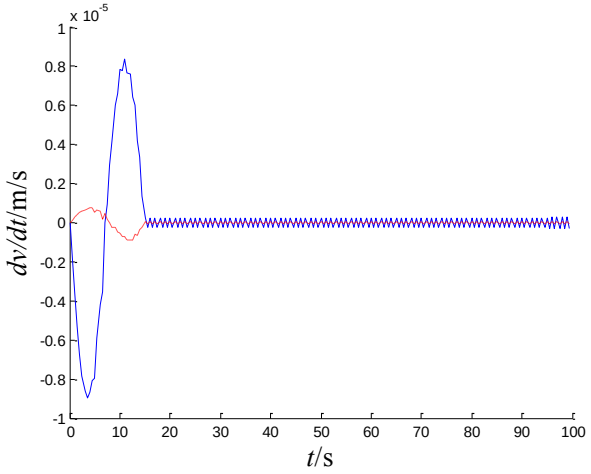


Figure 11: Speed change of blade tip

From Fig.10, we can see the maximum displacement of the rotating blade with equal section was larger than that of the blade with variable cross-section. It indicated that it was more scientific to

design the wind turbine blades as variable section. From Fig.11, we can conclude that the blades with variable cross-section were more stable than those with equal cross-section.

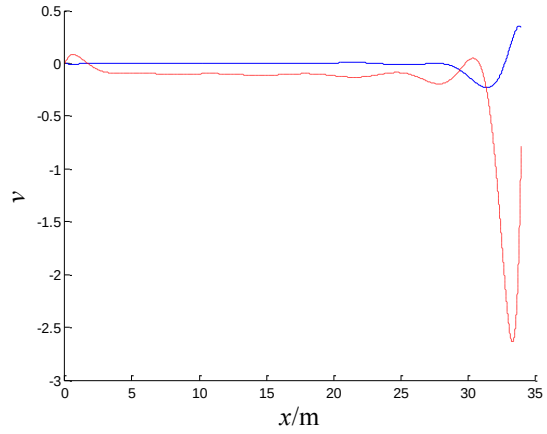


Figure 12: First modal shape chart

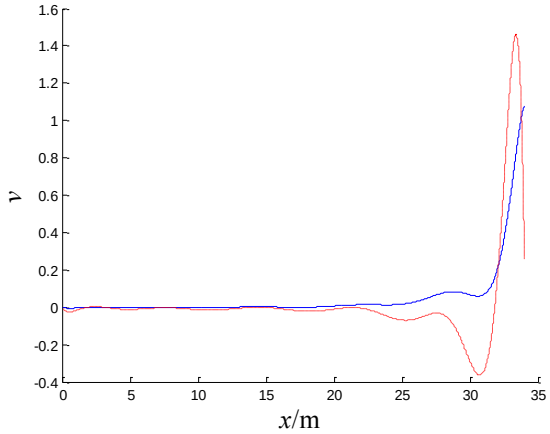


Figure 13: Two classes mode shapes chart

By comparing the first order and second order modes of the two kinds rotating blades, we can see from Fig.12 and Fig.13 that the dynamic response of the variable cross-section rotating blade was smaller and the variation trend was more stable.

If the pre-twist angle was further considered, we can get the simulation result as below.( blue line: blade with pre-twist angle, black line: non-pre-twist angle blade)

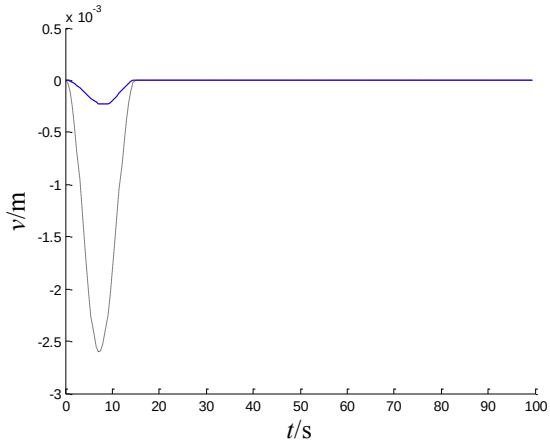


Figure 14:Displacement response of blade tip

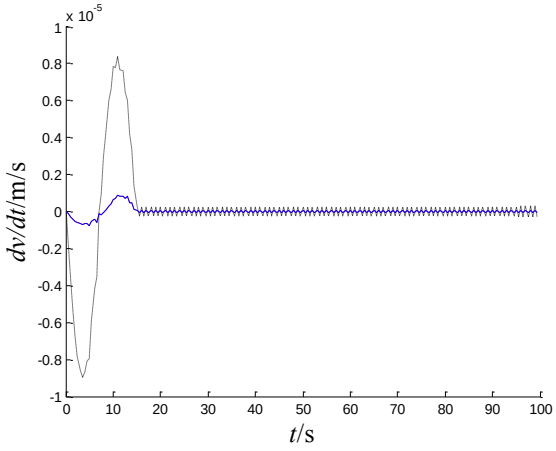


Figure 15: Speed change of blade tip

As we can see in Fig.14 and Fig.15, the displacement and speed of blade tip with pre-twist angle were smaller than the non-pre-twist angle rotating blade, this indicated that the pre-twisted blade should be more stable when there was a excitation.

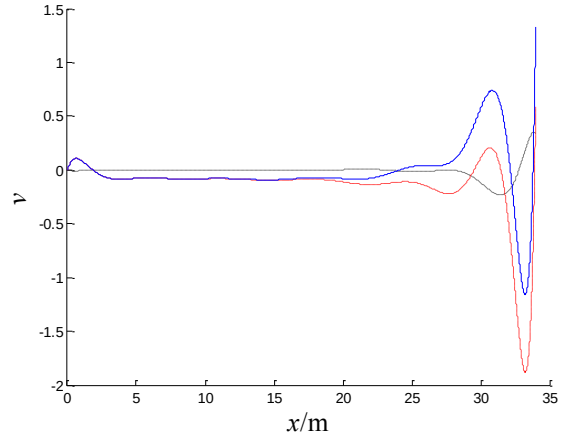


Figure 16: First modal shape chart

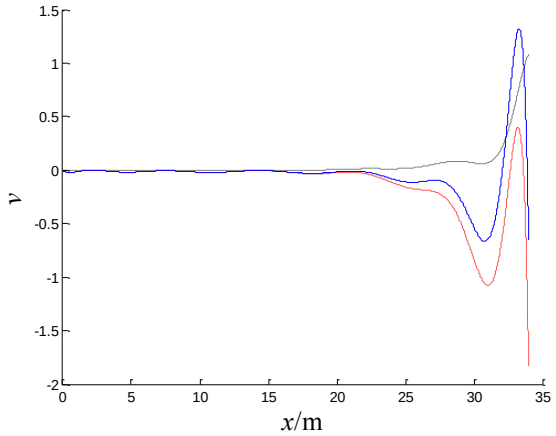


Figure 17: Two classes mode shapes chart

The simulation results showed that the curvature degree of the rotating blade with pre-twisting angle was less, its first two natural frequencies were larger than the non-pre-twist angle rotating blade, this means that rotating blades with a pre-twist angle will be more conducive to deal with a variety of working environment.

## 4. Summary

In this paper, based on the second Lagrange equations and finite element method, the effects of physical factors such as blade rotational speed, variable cross-section and pre-twist angle were analysed. Then the simulation results showed that a variable cross-section blade with pre-twist angle will be more suitable for engineering practice.

## 5. Acknowledgements

This paper is funded by the International Exchange Program of Harbin Engineering University for Innovation-oriented Talents Cultivation

## REFERENCES

1 H,Yoo, J. Chung, Dynamic analysis of a rotating cantilever, Journal of Sound and Vibration. (2002) 249(1), 147-164.

2 H,Yoo ,S.H.Shin, Vibration analysis of a rotating cantilever beams, Journal of Sound and Vibration.(1998) 212(5), 807-82.

3 Stafford R.O., Giiurgiutiu V. Semi-analytic methods of rotating Timoshenko beams. Journal of Mechanics＆Science.1975, 17:719-727.

4 T. Yokoyama. Free vibration characteristics of rotating Timoshenko beams. ASME Journal of Applied Mechanics.1986, 53:869-872.

5 Hodges D.H. On the extensional vibrations of rotating bars. Journal of Non-Linear Mechanics.1997, 12:293-296.

6 H. Yang J. Hong, Z. Yu, Dynamics modeling of a flexible hub-beam system with a tip mass [J].Journal of Sound and Vibration .266(4) (2003)759-774.

7 X. Tong, B, Tabarrok , K. Y. Yeh . Vibration analysis of Timoshenko beams with non-homogeneity and varying cross-section [J].Journal of Sound and Vibration 186(5)(1995)821-835.

8 H, Yoo , R, Ryan , R, Scott , Dynamics of flexible beams undergoing overall motions[J].Journal of Sound and Vibration 181(1995)261-278.